sustainability

MDPI

Article

Optimal Phase-Balancing in Three-Phase Distribution Networks Considering Shunt Reactive Power Compensation with Fixed-Step Capacitor Banks

Daniel Federico A. Medina-Gaitán [1], Ian Dwrley Rozo-Rodriguez [1] and Oscar Danilo Montoya [1,2,*]

[1] Grupo de Compatibilidad e Interferencia Electromagnética (GCEM), Facultad de Ingeniería, Universidad Distrital Francisco José de Caldas, Bogotá 110231, Colombia
[2] Laboratorio Inteligente de Energía, Facultad de Ingeniería, Universidad Tecnológica de Bolívar, Cartagena 131001, Colombia
* Correspondence: odmontoyag@udistrital.edu.co

Abstract: The black hole optimization (BHO) method is applied in this research to solve the problem of the optimal reactive power compensation with fixed-step capacitor banks in three-phase networks considering the phase-balancing problem simultaneously. A master–slave optimization approach based on the BHO in the master stage considers a discrete codification and the successive approximation power flow method in the slave stage. Two different evaluations are proposed to measure the impact of the shunt reactive power compensation and the phase-balancing strategies. These evaluations include a cascade solution methodology (CSM) approach and a simultaneous solution methodology (SSM). The CSM approach solves the phase-balancing problem in the first stage. This solution is implemented in the distribution network to determine the fixed-step capacitor banks installed in the second stage. In the SSM, both problems are solved using a unique codification vector. Numerical results in the IEEE 8- and IEEE 27-bus systems demonstrate the effectiveness of the proposed solution methodology, where the SSM presents the better numerical results in both test feeders with reductions of about 32.27% and 33.52%, respectively, when compared with the CSM. To validate all the numerical achievements in the MATLAB programming environment, the DIgSILENT software was used for making cross-validations. Note that the selection of the DIgISLENT software is based on its wide recognition in the scientific literature and industry for making quasi-experimental validations as a previous stage to the physical implementation of any grid intervention in power and distribution networks.

Keywords: phase-balancing problem; shunt reactive compensation; black hole optimization; successive approximations; power flow solution; cascade solution methodology; simultaneous solution methodology

Citation: Medina-Gaitán, D.F.A.; Rozo-Rodriguez, I.D.; Montoya, O.D. Optimal Phase-Balancing in Three-Phase Distribution Networks Considering Shunt Reactive Power Compensation with Fixed-Step Capacitor Banks. *Sustainability* **2023**, *15*, 366. https://doi.org/10.3390/su15010366

Academic Editor: Thanikanti Sudhakar Babu

Received: 24 November 2022
Revised: 21 December 2022
Accepted: 22 December 2022
Published: 26 December 2022

1. Introduction

1.1. General Context and Motivation

In the last two decades, population growth and technological advances have caused a considerable increase in the use of electrical energy at all voltage levels for residential, industrial, and commercial applications [1,2]. Because they directly connect end users and the electricity service, electrical distribution networks are the systems with the most accelerated growth compared to large-scale power and generation systems [3,4]. Due to the operating values of medium-voltage distribution networks, typically between 1 and 25 kV, these networks exhibit higher power loss percentages than transmission and subtransmission systems. These energy losses in distribution grids can be between 6 and 18% of the energy purchased at the terminals of the substation, whereas transmission systems show values between 1.5 and 2.5% [5].

On the other hand, given the policies implemented by the regulatory entities of the electrical sector, the values regarding energy losses in distribution networks must be continuously reduced by utilities to improve the quality, and the distribution efficiency of electrical energy [6,7]. To this effect, utilities need to design efficient maintenance and operation plans that allow for reaching the expected energy losses with minimal investment costs [8,9].

Due to the diversity of alternatives to improve the efficiency of the electrical service, distribution companies can select one or more of the following options to reduce their energy losses in distribution systems. The first alternative, valid for three-phase networks, involves using shunt reactive power compensators with fixed-capacitor banks or static var compensators [10,11]. The second option is using dispersed generation sources and battery energy storage systems. However, their costs are very high when compared to the first alternative, and the main application of distributed sources and batteries is related to active energy support to reduce energy purchasing costs for planning periods that oscillate between 5 and 20 years [12], not to reduce the energy losses during distribution activity. A detailed study regarding the optimal integration of renewable generation in distribution networks using multi-objective optimization was presented by the authors of [13], which constitutes an essential reference to understand the importance of having a multi-criteria decision algorithm to install dispersed generation sources in hybrid AC–DC distribution grids from economic and technical perspectives. The third option is an efficient grid reconfiguration, i.e., modifying the grid topology by using available tie-lines [14]. The final alternative corresponds to the optimal phase balancing, i.e., the redistribution of the load connections at all the network nodes to reduce excessive voltage drops in charged phases and the magnitude of the current in these phases [5].

This research proposes an efficient alternative to minimize the total grid power/energy losses based on the above-mentioned options. To this effect, the two cheapest options were selected, i.e., the optimal selection and location of fixed-step capacitor banks combined with optimal phase-swapping in all the network nodes.

1.2. State of the Art

In the literature, many approaches focus on integrating fixed-step capacitor banks into electrical distribution networks and solving the optimal phase-swapping problem in three-phase asymmetric networks. This subsection presents some of the most recent works in those areas.

1.2.1. Optimal Placement of Fixed-Step Capacitor Banks

The authors of [15] presented a solution methodology for the optimal selection and location of fixed-step capacitor banks in medium-voltage distribution grids, intending to reduce grid power losses and improve the voltage profiles. The proposed methodology was based on applying the crow search algorithm, a bio-inspired combinatorial optimization methodology. Numerical results were obtained in two test feeders composed of 9 and 33 buses, with better solutions when compared to the classical particle swarm optimization (PSO) method. The work by [16] presented an interesting case study associated with installing capacitor banks in a distribution network that provides energy service to the Tehran metro. The main characteristic of this approach is the use of the ETAP software and its optimization tool concerning the optimal placement of capacitor banks through the implementation of a specialized genetic algorithm, which minimizes the total investment costs in compensators for an expected analysis period. Numerical results showed that, for a planning period of 5 years, the cumulative net profit regarding the reduction of energy losses costs while considering the capacitors' investment and operating costs amounts to more than 300,000 dollars. These results revealed the positive impact of using fixed-step capacitor banks to improve performance in electrical distribution networks with bad lagging power factors. The work by [10] proposed the application of the whale optimization algorithm to locate and select fixed-step capacitor banks in radial distribution grids. The

optimization process considered two objective functions regarding operating cost reduction and power loss minimization. The IEEE 34-bus grid and the IEEE 85-bus grid were selected as test feeders to validate the effectiveness of the proposed optimization approach in comparison with the methods reported in the literature, such as the PSO method, the plant growth simulation algorithm, and the bacterial foraging optimization algorithm, among others. The authors of [17] presented the application of the flower pollination algorithm to locate and select fixed-step capacitor banks in radial distribution networks to minimize the annual costs of energy losses while including the investment costs of the capacitor banks. Numerical results in the IEEE 33-, 34-, 69-, and 85-node grids demonstrated the effectiveness of the proposed optimization algorithm when compared to an analytical method and an improved fuzzy-logic genetic algorithm. The study by [18] applied the cuckoo search algorithm to locate and size fixed-step capacitor banks in radial distribution networks. The IEEE 34- and 69-bus grids were employed in all numerical validations. The objective was to minimize the total grid power losses and improve the voltage profiles along the distribution feeder. A comparative analysis with the classical PSO approach and the plant growth simulation algorithm demonstrated the effectiveness of the cuckoo search algorithm in solving the studied problem. Additional optimization algorithms to locate and capacitor banks are the hybrid honey bee colony algorithm [19], the tabu search algorithm [20,21], the vortex search algorithm [22], and the gravitational search algorithm [23], among others. In the case of three-phase asymmetric distribution grids, the authors of [24] presented the application of the imperialist competitive algorithm to locate and size capacitor banks while considering three-phase networks with harmonic pollution. The work by [25] presented the effect of an unbalanced grid regarding the presence of single-, two-, and three-phase loads on the final location and size of fixed-step capacitor banks while considering the minimization of the total grid power losses and the reduction of voltage imbalances.

The works mentioned above have two main characteristics: (i) the use of combinatorial optimization techniques (i.e., metaheuristics) to deal with the nonlinearities and non-convexities of the exact mixed-integer nonlinear programming model that represents the studied problem; and (ii) the fact that most of the optimization approaches use single-phase equivalents for the distribution grid modeling. This means that more research is required regarding asymmetric distribution networks.

1.2.2. Optimal Phase-Balancing in Three-Phase Asymmetric Grids

The authors of [26] presented the application of a specialized Chu and Beasley genetic algorithm to solve the problem regarding optimal phase-balancing in three-phase asymmetric networks with multiple constant power loads. Numerical results in the IEEE 37-bus grid demonstrate the effectiveness of the proposed genetic algorithms. However, no comparisons with other optimization methods were reported. The work by [27] presented the application of a mixed-integer approximation to solve the optimal load balancing problem in three-phase distribution networks while using a current approximation method. The study by [5] proposed the application of the vortex search algorithm to solve the optimal phase-balancing problem in three-phase distribution networks while aiming to minimize the expected value of the grid power losses. The IEEE 8-, 25-, and 37-bus grids were used as test feeders. Numerical comparisons with the classical Chu and Beasley genetic algorithm demonstrated the effectiveness of the proposed vortex search algorithm in minimizing the objective function. The authors of [28] presented a heuristic optimization algorithm based on measuring the phase current at the point of load connection. With these measurements, each load is reconfigured to minimize the expected current imbalance. Numerical results and comparisons with the phase commitment algorithm and the modified leap frog optimization method confirmed the proposal's effectiveness in test feeders composed of 8, 15, and 30 asymmetric loads. The study by [29] presented the solution of the optimal phase-balancing problem in three-phase asymmetric networks operated at low voltage levels (i.e., secondary distribution networks). The IEEE 13-node test feeder was selected to

evaluate the heuristics-based solution proposal. However, no comparisons with literature reports were presented. The authors of [30] proposed applying artificial intelligence-based methods using artificial neural networks that consider information provided by smart meters. The main contribution of this paper was the application of neural networks to an actual distribution feeder belonging to the Irbid district electricity company. The work by [31] proposed applying the hurricane optimization algorithm to solve the optimal phase-swapping problem in three-phase asymmetric networks. The objective function corresponded to minimizing the total grid power losses under peak load conditions. The IEEE 8-, 25-, and 37-bus grids were employed for numerical validations. A comparative analysis with the Chu and Beasley genetic algorithm and the vortex search algorithm demonstrated the effectiveness of the proposed optimization method regarding the final power loss value.

Note that most of the optimization methods mentioned above for solving the problem under study are based on applying combinatorial optimization algorithms (metaheuristics) to obtain a high-quality solution, which implies that the application of recently developed combinatorial algorithms shows excellent promise for research in this field, as is the case of the black hole optimization (BHO) technique used in this work.

1.3. Contribution and Scope

Considering the above, no solution methodologies in the current literature simultaneously address the problems regarding phase-balancing and reactive power compensation. Thereupon, this work makes the following contributions:

i. A complete comparative analysis regarding reactive power compensation with fixed-step capacitor banks and the phase-balancing approach to reduce peak power losses in distribution grids by presenting cascade and simultaneous solution methodologies;
ii. The application of the BHO method to determine the size and location of the capacitors, as well as the best set of load connections in three-phase nodes, using a discrete codification.

It is worth mentioning that this research only considers an objective function based on the minimization of a technical aspect of the distribution grid, i.e., the expected power losses under peak load conditions. In addition, the selection of test feeders for validating the proposed optimization method is based on the literature reports where the studied problems were solved separately. In addition, note that the selection of the BHO approach is based on simple evolution rules and is highly efficient in solving combinatorial optimization problems, added to the fact that, according to our exploration of the literature, this algorithm has not been applied to solve both studied optimization problems using cascade or simultaneous solution methodologies, which has been identified as a research gap to be filled by this work. On the other hand, it is essential to acknowledge the strong connection between sustainability and the issue under study, given that part of the electrical energy converted into heat in distribution lines is obtained from fossil fuels. Reducing this makes distribution networks more sustainable, as less damaged energy resources are required to provide electrical energy to all end users connected to those grids.

1.4. Document Structure

The remainder of this research document is structured as follows: Section 2 presents a general formulation of the load flow problem for three-phase asymmetric distribution networks, which is based on the three-phase version of the successive approximations power flow method; Section 3 presents the general characteristics of the mathematical models regarding the optimal location of the fixed-step capacitor banks and optimal phase-swapping in three-phase grids; Section 4 describes the general aspects of the BHO technique by presenting its general conception, mathematical formulation, and algorithmic implementation; Section 5 shows the main characteristics of the distribution systems under analysis, as well as the parametrization regarding the sizes of the fixed-step capacitor banks; Section 6 presents all the numerical validations in the 8- and 25-bus grids, with a complete

analysis and discussion; and Section 7 lists the main conclusions derived from this work, as well as some possible future works.

2. Load Flow Analysis

This section presents the main aspects of the power flow problem for three-phase unbalanced networks. A detailed description of a recently developed power flow approach based on the successive approximations power flow method is provided, as it is at the heart of any combinatorial optimization method applied to improve the performance of electrical networks.

The load flow problem is one of the most classical problems in the field. It has been studied for six decades and is related to determining the steady-state conditions of an electrical network when it has at least one slack source and multiple constant power loads [32]. The solution of the power flow problem in three-phase distribution networks with asymmetric loads, as well as the case of single-phase systems, requires the application of numerical methods and a set of nonlinear equality constraints involved in this problem [33]. Once the load flow problem has been solved, it is possible to determine all the electrical characteristics of the electrical network under analysis, i.e., the total grid losses, the maximum voltage regulation, and the maximum loadability in the transmission/distribution lines, among others [34]. This research adopts the successive approximations method for solving the load flow in three-phase asymmetric networks, as reported by [5]. The main characteristics of this power flow method are as follows:

i. It is a derivative-free load flow method and corresponds to a generalization of the classical backward/forward load flow method;
ii. The convergence of the successive approximations method is linear due to the absence of derivatives in its formulation;
iii. By applying Banach's fixed-point theorem, it is possible to ensure its convergence to the load flow solution if and only if the distribution grid operates far from the voltage collapse point [35].

The formulation of the successive approximations load flow method for general three-phase asymmetric distribution grids starts with the general definition of complex power (Tellegen's second theorem) for a generic node k, as defined by (1):

$$S_k = \text{diag}(V_k) I_k^*, \tag{1}$$

where S_k is the complex average power consumption at node k, which has a complex voltage V_k, and a net current injection I_k. Note that A^* represents the conjugate value of the complex variable/parameter A, and $\text{diag}(B)$ is an operator that makes the vector B a diagonal matrix. If the conjugate operator is taken on both sides of (1), then the following equivalent equation is obtained:

$$S_k^* = \text{diag}(V_k^*) I_k. \tag{2}$$

According to [36], the relationship between currents and voltages for a three-phase system is given by the following equations:

$$I_k^{abc} = \left[Y_k^{abc} \right] V_k^{abc}, \tag{3}$$

where V_k^{abc}, I_k^{abc}, and Y_k^{abc} are defined as follows:

$$V_k^{abc} = \begin{bmatrix} V_k^{(a)} \\ V_k^{(b)} \\ V_k^{(c)} \end{bmatrix}, \tag{4}$$

$$I_k^{abc} = \begin{bmatrix} I_k^{(a)} \\ I_k^{(b)} \\ I_k^{(c)} \end{bmatrix}, \tag{5}$$

$$Y_k^{abc} = \begin{bmatrix} Y_k^{(aa)} & Y_k^{(ab)} & Y_k^{(ac)} \\ Y_k^{(ba)} & Y_k^{(bb)} & Y_k^{(bc)} \\ Y_k^{(ca)} & Y_k^{(cb)} & Y_k^{(cc)} \end{bmatrix}, \tag{6}$$

where $V_k^{(a)}$, $V_k^{(b)}$, and $V_k^{(c)}$ are the a-, b-, and c-phase voltages at node k; $I_k^{(a)}$, $I_k^{(b)}$, and $I_k^{(c)}$ are the net injected currents in phases a, b, and c at node k; and Y_k^{abc} represents the nodal admittance matrix that relates phases a, b, and c at node k.

Suppose that the definitions of the three-phase variables in (4) and (5) are replaced into the general complex power of node k in (2). In that case, the general expression for the three-phase complex power is obtained as presented below:

$$S_k^{abc} = \text{diag}\left(V_k^{abc}\right) I_k^{abc,*}. \tag{7}$$

In addition, if the nodal admittance matrix (6) is substituted into (7), the results of (8) and (9) yield the following:

$$S_k^{abc} = \text{diag}\left(V_k^{abc}\right) \left[Y_k^{abc,*}\right] V_k^{abc,*}, \tag{8}$$

$$S_k^{abc,*} = \text{diag}\left(V_k^{abc,*}\right) \left[Y_k^{abc}\right] V_k^{abc}. \tag{9}$$

For the analysis of our load flow, the nodes are classified into generation nodes (g) and load or demand nodes (d), where the slack node is taken as the generating node and the rest as demand nodes. With this in mind, the following formulation can be made:

$$\begin{bmatrix} I_g \\ I_d \end{bmatrix} = \begin{bmatrix} Y_{gg} & Y_{gd} \\ Y_{dg} & Y_{dd} \end{bmatrix} \begin{bmatrix} V_g \\ V_d \end{bmatrix} \tag{10}$$

where I_g is a complex variable that contains the net current injection in the generation node, I_d is a complex vector that contains all the demanded currents of the network, V_g is a complex variable that contains the voltage output of the generation source, and V_d is a complex vector that contains all the demanded voltages in the consumption nodes. Now, by substituting the definition in (10) into (9), the following set of general equalities is found:

$$S_g^{abc,*} = \text{diag}\left(V_g^{abc,*}\right) \left[Y_{gg}^{abc} V_g^{abc} + Y_{gd}^{abc} V_d^{abc}\right], \tag{11}$$

$$-S_d^{abc,*} = \text{diag}\left(V_d^{abc,*}\right) \left[Y_{dg}^{abc} V_g^{abc} + Y_{dd}^{abc} V_d^{abc}\right], \tag{12}$$

where S_g^{abc} and $|S_d^{abc}|$ are the apparent powers of phases a, b, and c generated by the slack node, as well as the apparent power of phases a, b, and c consumed by the load nodes, respectively; $|V_g^{abc}|$ is the three-phase voltage output of the generation sources, and $|V_d^{abc}|$ is a complex vector with all the unknown voltages of the remaining nodes. It is worth noting that the negative sign in (12) is associated with the direction of the injected power, as it leaves the demand nodes and arrives at the generation nodes.

Now, if what is described in (12) is mathematically reorganized, it is possible to determine the unknown voltage for each load node:

$$V_d^{abc} = -\left[Y_{dd}^{abc}\right]^{-1} \left[\text{diag}\left(V_d^{abc,*}\right)^{-1} S_d^{abc,*} + Y_{dg}^{abc} V_g^{abc}\right] \tag{13}$$

Due to the nonlinear structure of Equation (13), it is necessary to implement an iterative process to reach a numerical solution with an acceptable convergence (ε).

$$V_d^{(abc,t+1)} = -\left[Y_{dd}^{abc}\right]^{-1}\left[\text{diag}\left(V_d^{abc,*,t}\right)^{-1} S_d^{abc,*} + Y_{dg}^{abc} V_g^{abc}, |\right] \tag{14}$$

where t is defined as the iterative counter, and the evaluation of the recursive formula reaches convergence when the criterion in (15) is met:

$$\max\left|\left|V_d^{abc,t+1}\right| - \left|V_d^{abc,t}\right|\right| \leq \varepsilon \tag{15}$$

As recommended by [5], the value assigned for the ε-parameter is 1×10^{-10}.

3. Phase-Balancing and Fixed Capacitor Banks in Distribution Grids

This section describes the main aspects of the problems regarding phase-balancing and optimal reactive power injection with fixed-step capacitor banks in asymmetric three-phase distribution networks.

3.1. Phase-Balancing Problem

In three-phase asymmetric distribution networks, one of the most common problems concerns the current imbalances along the distribution feeder and the voltage imbalances in the demand nodes [37]. This is due to the presence of multiple single-, two-, and three-phase loads along the distribution grid, which are not adequately connected to the grid, i.e., without considering an efficient expansion/operation plan [38].

To deal with the problems caused by load imbalances in three-phase distribution networks, one of the most widely known and cheapest alternatives is optimal phase-balancing using mathematical optimization [5]. In three-phase systems, for a general three-phase load, there are six different possible connections $\left(H_{(i)}\right)$ between phases a, b, and c. These configurations are listed in Table 1.

Table 1. Possible load connections in a particular node.

Index H_i	Connection	Sequence
1	ABC	No change
2	BCA	
3	CAB	
4	ACB	Change
5	CBA	
6	BAC	

Remark 1. *The main characteristic of the type of load connections in Table 1 is that the first three connections are defined in a positive sequence, and the other three in a negative sequence, which means that one must check whether there are rotating machines at the points of load connection. In this sense, an inversion of the input voltage sequence can damage these devices due to torque inversion [26].*

The main idea of optimal phase-swapping in three-phase asymmetric networks is to minimize the expected power losses under particular load conditions. These power losses can be calculated via Equation (16):

$$\min p_{\text{loss}} = \text{real}\left\{\sum\left(S_g^{abc} - S_d^{abc}\right)\right\}, \tag{16}$$

where p_{loss} is the expected value of the power losses, calculated as the difference between the power generation and power consumption.

The minimization of the power losses defined in (16) is subject to the expected electrical behavior of the distribution network under analysis, which is determined by the active and reactive power balance at each node and phase of the distribution grid. These are defined generically in Equations (17) and (18). In addition, the voltage regulation limits are defined in inequality constraint (19):

$$P\left(V_k^{abc}, \Theta_k^{abc}, V_m^{abc}, \Theta_m^{abc}, Y_k^{abc}, Y_m^{abc}, H\right) = 0, \tag{17}$$

$$Q\left(V_k^{abc}, \Theta_k^{abc}, V_m^{abc}, \Theta_m^{abc}, Y_k^{abc}, Y_m^{abc}, H\right) = 0, \tag{18}$$

$$V_k^{abc,\min} \leq V_k^{abc} \leq V_k^{abc,\max}. \tag{19}$$

Note that Equations (17) and (18) represent the general active and reactive power balance constraints at each node k at each one of the phases, which are functions of the voltage variables V_k^{abc} and V_m^{abc}, their angles Θ_k^{abc} and Θ_m^{abc}, and the parametric information of the distribution network (i.e., the admittance matrices Y_k^{abc} and Y_m^{abc}, and the load connections H defined in Table 1).

Remark 2. *The solution of the optimization model (16)–(19) requires the application of efficient optimization methods due to the intrinsic nonlinear, non-convex characteristics of the active and reactive power balance equations, as well as the inclusion of integer variables to represent each possible load connection at each node of the three-phase asymmetric distribution grid.*

In this research, the set of load connections at each node (i.e., the values of the variables H_i) is defined by applying the black hole optimizer while using a discrete codification.

3.2. Capacitor Banks

The optimal placement of capacitor banks in electrical distribution networks, in conjunction with solving the optimal phase-balancing problem, is one of the most common and cheapest approaches to reducing the expected cost of the energy losses in distribution grids [10]. An additional advantage of including capacitor banks for reactive power compensation in distribution grids is that these devices also contribute to voltage profile improvements along the distribution feeder, especially in nodes far from the substation bus [15].

The main characteristic of installing capacitor banks in distribution networks is using fixed reactive power compensation values. This research employs the parametric information reported by [10], where capacitors with sizes of 150 kvar are implemented while considering the possibility of installing 0 to 12 per node in parallel (see the sizes of the capacitors in Table 2).

Table 2. Set of possible sizes for the capacitor banks.

Capacitor Banks												
Bank	1	2	3	4	5	6	7	8	9	10	11	12
Size	150	300	450	600	750	900	1050	1200	1350	1500	1650	1800

Equation (20) presents the final value of the set of capacitor banks located at node k, defined as $VRC_{(k)}$:

$$VRC_{(k)} = nQ_{(c)}, \tag{20}$$

where n is the number of capacitor banks connected in parallel, each of them with a size of $Q_{(c)} = 150$ kvar.

Once the sizes of the set of capacitor banks that will be connected to the node k are known, they must be subtracted from the reactive power consumption of these nodes to quantify their effect in terms of power losses by using the three-phase power flow solution

presented in Section 2. The new reactive power demand in the nodes where the capacitor banks must be placed is presented in Equation (21):

$$\begin{bmatrix} Q_{Dk}^{(a)} \\ Q_{Dk}^{(b)} \\ Q_{Dk}^{(c)} \end{bmatrix} = \begin{bmatrix} Q_{dk}^{(a)} - VRC_{(k)} \\ Q_{dk}^{(b)} - VRC_{(k)} \\ Q_{dk}^{(c)} - VRC_{(k)}, \end{bmatrix} \quad (21)$$

where $Q_{dk}^{(a)}$, $Q_{dk}^{(b)}$, and $Q_{dk}^{(c)}$ correspond to the reactive power demand values for phases a, b, and c at node k, respectively; and $Q_{Dk}^{(a)}$, $Q_{Dk}^{(b)}$, and $Q_{Dk}^{(c)}$ correspond to the value of reactive power demanded by phases a, b, and c in node k after placing and connecting the fixed-step capacitor banks.

Remark 3. *Note that, to determine the best set of capacitor banks that must be installed at each node k, it is necessary to implement efficient optimization methods, given the discrete nature of the solution space and the nonlinear relation with the active and reactive power constraints in the power flow problem.*

In this research, the set of capacitor banks (i.e., the values of the variables $RC_{(k)}$), is defined by applying the black hole optimizer while using a discrete codification.

4. Solution Methodology Based on the BHO Approach

Bio-inspired computing is a field of study based on natural phenomena that seek to solve complex optimization problems [39]. At present, the complexity of optimization problems is increasing almost exponentially, which makes it increasingly challenging to solve said problems using classical algorithms. This has motivated the research and development of bio-inspired optimization algorithms [40].

The BHO algorithm is a bio-inspired metaheuristic method based on the dynamic interaction that exists between the center of a black hole and the cosmic matter transiting around it, whose purpose is to solve large nonlinear optimization problems by using simple mathematical formulas [41,42]. BHO was introduced in 2013 by [43], who illustrated it as an iterative method based on population, where the best candidate solution is selected as the *black hole* and the rest of the candidates are the cosmic matter revolving around it, i.e., *stars*.

This research considers two optimization strategies to solve the problems regarding optimal phase-balancing and optimal reactive power compensation in three-phase asymmetric distribution networks: the cascade optimization method and the simultaneous optimization approach.

i. Cascade solution methodology (CSM): The cascade optimization approach consists of a sequential solution of the studied optimization problems. First, the BHO method is applied to define the best set of load connections in all the nodes of the network, i.e., to solve the optimal phase-swapping problem. Second, fixing the solution of the phase-balancing problem, BHO is applied once again to obtain the set of fixed-step capacitor banks that will be connected to the three-phase nodes. The final solution corresponds to the grid power losses after locating and sizing the set of capacitor banks.
ii. Simultaneous solution methodology (SSM): The simultaneous solution strategy consists of using a unified codification to represent the problems regarding optimal phase-swapping and the optimal location of fixed-step capacitor banks with a single vector. Each candidate solution is evaluated with the three-phase power flow approach in order to determine the final value of the grid power losses. The final solution corresponds to the black hole's location with the best load connections and capacitor sizes, i.e., the minimum value for the grid power losses.

Both of the proposed solution methodologies, which are based on applying the BHO method, are explained in Algorithms 1 and 2.

Algorithm 1 Cascade solution methodology

Stage 1
Data: BHO parameters and test feeder information.
for t_1 = 1:t_{max} **do**
  if $t_1 == 1$ **then**
    Generate the initial population of stars for the phase-balancing problem;
    Evaluate each star with the three-phase power flow algorithm;
    Determine the expected power losses for each star (objective function value);
    Establish the position of the black hole (best current solution)
  else
    Generate the descending population for the new set of load connections;
    Evaluate each new star in the three-phase power flow algorithm;
    Determine the expected power losses for each star (objective function value);
    Update black hole position;
    Replace the stars absorbed by the black hole;
  end if
end for
Stage 2
Data: Fix the solution of the phase-balancing problem and define the set of capacitor banks available
for t_2 = 1:t_{max} **do**
  if $t_2 == 1$ **then**
    Generate the initial population of stars for the capacitor sizing and location problem;
    Evaluate each star with the three-phase power flow algorithm;
    Determine the expected power losses for each star (objective function value);
    Establish the position of the black hole (best current solution)
  else
    Generate the descending population for the new set of capacitor banks;
    Evaluate each new star in the three-phase power flow algorithm;
    Determine the expected power losses for each star (objective function value);
    Update black hole position;
    Replace the stars absorbed by the black hole;
  end if
end for

Algorithm 2 Simultaneous solution methodology

Data: BHO parameters and test feeder information.;
for t : 1 = 1:t_{max} **do**
  if $t_1 == 1$ **then**
    Generate the initial population of stars for the phase-balancing and capacitor sizing and location problems;
    Evaluate each star with the three-phase power flow algorithm;
    Determine the expected power losses for each star (objective function value);
    Establish the position of the black hole (best current solution)
  else
    Generate the descending population for the new set of load connections and capacitor sizes and locations;
    Evaluate each new star with the three-phase power flow algorithm;
    Determine the expected power losses for each star (objective function value);
    Update black hole position;
    Replace the stars absorbed by the black hole;
  end if
end for

Remark 4. *The detailed aspects of the implementation of the BHO method (i.e., evolution rules, black hole updating, and stars replacement, among others) can be consulted in [43].*

5. Test Feeders

This section presents the main characteristics of the test feeders used for validating the solution methodologies: IEEE 8- and 25-bus grids. Both networks are asymmetric and highly unbalanced. The main characteristics of these networks are described below.

5.1. IEEE 8-Bus Grid

The IEEE 8-bus grid is composed of a slack node located at node 1 and seven demand nodes, all connected by seven lines with a radial structure [5]. This test feeder operates with a medium voltage value of 11 kV and total per-phase active and reactive power values of 1005 kW and 485 kvar, 785 kW and 381 kvar, and 1696 kW and 821 kvar. The electrical configuration of this test feeder is depicted in Figure 1.

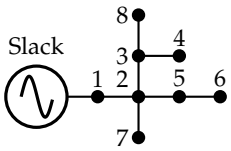

Figure 1. Single-phase diagram of the IEEE 8-bus system.

The parametric information regarding three-phase loads and impedances for the IEEE 8-bus grid is presented in Tables 3 and 4.

Table 3. Load information and conductor types for the IEEE 8-bus system.

Line	Node i	Node j	Conductor	Lenght (Ft)	P_{jA} (kW)	Q_{jA} (kvar)	P_{jB} (kW)	Q_{jB} (kvar)	P_{jC} (kW)	Q_{jC} (kvar)
1	1	2	1	5280	519	250	259	126	515	250
2	2	3	2	5280	0	0	259	126	486	235
3	2	5	3	5280	0	0	0	0	226	109
4	2	7	3	5280	486	235	0	0	0	0
5	3	4	4	5280	0	0	0	0	324	157
6	3	8	5	5280	0	0	267	129	0	0
7	5	6	6	5280	0	0	0	0	145	70

Table 4. Impedance matrix per type of conductor in the IEEE 8-bus grid.

Conductor (Ω/mi)			
1	0.093654 + 0.0429300i 0.031218 + 0.0134310i 0.031218 + 0.0134310i	0.031218 + 0.0134310i 0.093654 + 0.0402930i 0.031218 + 0.0134310i	0.031218 + 0.0134310i 0.031218 + 0.0134310i 0.093654 + 0.0402930i
2	0.156090 + 0.0671550i 0.052030 + 0.0223850i 0.052030 + 0.0223850i	0.052030 + 0.0223850i 0.156090 + 0.0671550i 0.052030 + 0.0223850i	0.052030 + 0.0223850i 0.052030 + 0.0223850i 0.156090 + 0.0671550i
3	0.046827 + 0.0201465i 0.015609 + 0.0067155i 0.015609 + 0.0067155i	0.015609 + 0.0067155i 0.046827 + 0.0201465i 0.015609 + 0.0067155i	0.015609 + 0.0067155i 0.015609 + 0.0067155i 0.046827 + 0.0201465i
5	0.062436 + 0.0268620i 0.020812 + 0.0089540i 0.020812 + 0.0089540i	0.020812 + 0.0089540i 0.062436 + 0.0268620i 0.020812 + 0.0089540i	0.020812 + 0.0089540i 0.020812 + 0.0089540i 0.062436 + 0.0268620i
6	0.078045 + 0.0335775i 0.026015 + 0.0111925i 0.026015 + 0.0111925i	0.026015 + 0.0111925i 0.078045 + 0.0335775i 0.026015 + 0.0111925i	0.026015 + 0.0111925i 0.026015 + 0.0111925i 0.078045 + 0.0335775i

5.2. IEEE 25-Bus Grid

The IEEE 25-bus grid is a radial medium-voltage distribution network that operates at a voltage of 4.16 kV in terminals of the substation [44]. It has 25 nodes, 22 nodes with unbalanced loads, two step nodes, and one substation bus located at node 1. The electrical configuration of this test feeder is presented in Figure 2.

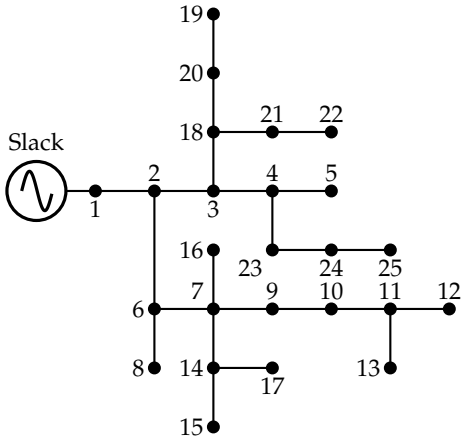

Figure 2. Single-phase diagram of the IEEE 25-bus system.

The parametric information regarding three-phase loads and impedances for the IEEE 25-bus grid is presented in Tables 5 and 6.

Table 5. Load information and conductor types for the IEEE 25-bus system.

Line	Node i	Node j	Conductor	Length (ft)	P_{jA} (kW)	Q_{jA} (kvar)	P_{jB} (kW)	Q_{jB} (kvar)	P_{jC} (kW)	Q_{jC} (kvar)
1	1	2	1	1000	0	0	0	0	0	0
2	2	3	1	500	36	21.6	28.8	19.2	42	26.4
3	2	6	2	500	43.2	28.8	33.6	24	30	30
4	3	4	1	500	57.6	43.2	4.8	3.4	48	30
5	3	18	2	500	57.6	43.2	38.4	28.8	48	36
6	4	5	2	500	43.2	28.8	28.8	19.2	36	24
7	4	23	2	400	8.6	64.8	4.8	3.8	60	42
8	6	7	2	500	0	0	0	0	0	0
9	6	8	2	1000	43.2	28.8	28.8	19.2	3.6	2.4
10	7	9	2	500	72	50.4	38.4	28.8	48	30
11	7	14	2	500	57.6	36	38.4	28.8	60	42
12	7	16	2	500	57.6	4.3	3.8	28.8	48	36
13	9	10	2	500	36	21.6	28.8	19.2	32	26.4
14	10	11	2	300	50.4	31.7	24	14.4	36	24
15	11	12	3	200	57.6	36	48	33.6	48	36
16	11	13	3	200	64.8	21.6	33.6	21.1	36	24
18	14	15	2	300	7.2	4.3	4.8	2.9	6	3.6
17	14	17	3	300	57.6	43.2	33.6	24	54	38.4
19	18	20	2	500	50.4	36	38.4	28.8	54	38.4
20	18	21	3	400	5.8	4.3	3.4	2.4	5.4	3.8
21	20	19	3	400	8.6	6.5	4.8	3.4	6	4.8
22	21	22	3	400	72	50.4	57.6	43.2	60	48
23	23	24	2	400	50.4	36	43.2	30.7	4.8	3.6
24	24	25	3	400	8.6	6.5	4.8	2.9	6	4.2

Table 6. Impedance matrix per type of conductor in the IEEE 25-bus grid.

Conductor (Ω/mi)			
1	0.3686 + 0.6852i 0.0169 + 0.1515i 0.0155 + 0.1098i	0.0169 + 0.1515i 0.3757 + 0.6715i 0.0188 + 0.2072i	0.0155 + 0.1098i 0.0188 + 0.2072i 0.3723 + 0.6782i
2	0.9775 + 0.8717i 0.0167 + 0.1697i 0.0152 + 0.1264i	0.0167 + 0.1697i 0.9844 + 0.8654i 0.0186 + 0.2275i	0.0152 + 0.1264i 0.0186 + 0.2275i 0.981 + 0.8648i
3	1.9280 + 1.4194i 0.0161 + 0.1183i 0.0161 + 0.1183i	0.0161 + 0.1183i 1.9308 + 1.4215i 0.0161 + 0.1183i	0.0161 + 0.1183i 0.0161 + 0.1183i 1.9337 + 1.4236i

6. Numerical Results

This section shows the results obtained when the BHO algorithm was implemented in the 8- and 25-node IEEE test systems for the cases described above, i.e., the required new configurations and locations of the capacitor banks.

To define the best parameters for the proposed BHO in the CSM and SSM cases, multiple evaluations in both test feeders were conducted, modifying the number of individuals in the population and the number of iterations. In addition, two different computers were used to corroborate the effectiveness of the optimization method. After these evaluations, the set of parameters selected for the BHO approach was 1000 iterations per evaluation and a dimension of the initial population equivalent to 30 stars.

6.1. Benchmark Case Evaluation

To corroborate that the three-phase power flow solution presented in Section 2 is efficient in solving the power flow problem, a comparative analysis was performed with benchmark cases in both test feeders, i.e., without optimal phase-balancing and capacitor connection, while using the DIgSILENT software with the Newton–Raphson method. Note that the selection of the DIgSILENT software for validating the power results is based on its wide acceptance in the current literature and the industry for power system studies, as it is considered to be a quasi-experimental validation [45,46]. Table 7 presents the power flow solution obtained by using the MATLAB programming environment and the DIgSILENT software.

Table 7. Comparison of power losses obtained using MATLAB and DIgSILENT in the benchmark cases for the IEEE 8- and IEEE 25-bus grids.

IEEE 8-Bus Grid				
Software	**Phase a (kW)**	**Phase b (kW)**	**Phase c (kW)**	**Total (kW)**
MATLAB	1.71579	2.33048	9.94624	13.99252
DIgSILENT	1.71579	2.32948	9.94869	13.99396
IEEE 25-bus grid				
MATLAB	36.88008	14.78598	23.75453	75.42059
DIgSILENT	36.88436	14.78348	23.75532	75.42315

The numerical results in Table 7 allow for confirming that the successive approximations power flow method presented in Section 2 is efficient in solving power flow problems in three-phase distribution grids. In comparison with the Newton–Raphson method available in the DIgSILENT software, less than 0.011% was obtained in both test feeders. This difference can be attributed to the convergence error that can be set for the Newton–Raphson in the DIgSILENT software, which is about 1×10^{-06}, whereas the MATLAB power flow was set with a convergence error of about 1×10^{-10}.

6.2. Results for the IEEE 8-Bus Grid

In this test feeder, the first evaluation concerned the effect of the CSM on the final grid power losses of the network. The first stage, as presented in Figure 1, is the solution to the optimal phase-swapping problem. Table 8 presents the solution to the phase-balancing problem using the BHO method and its evaluations in the DIgSILENT software.

Table 8. Power losses after solving the optimal phase-balancing problem in the IEEE 8-bus grid.

Software	Phase a (kW)	Phase b (kW)	Phase c (kW)	Total (kW)
MATLAB	3.84635	2.74121	3.99930	10.58686
DIgSILENT	3.84646	2.74103	3.99942	10.58691

Note that the comparison between MATLAB and DIgSILENT confirms the effectiveness of the proposed optimization method to redefine the load connections, reaching final power losses values of about 10.5868 kW, i.e., a reduction of 24.34% with respect to the benchmark case. It is worth mentioning that the solution reached by the BHO approach is equivalent to the solution reported in [5] with the application of the vortex search algorithm.

To verify the effect of integrating capacitor banks in three-phase asymmetric distribution grids, the BHO approach was implemented in order to locate these devices on the benchmark test system, i.e., without employing the phase-balancing approach. These results are listed in Table 9, including the comparison between the MATLAB power flow and the DIgSILENT one.

Table 9. Power losses after solving the problem regarding optimal reactive power compensation in the IEEE 8-bus grid.

Software	Phase a (kW)	Phase b (kW)	Phase c (kW)	Total (kW)
MATLAB	1.94536	1.54599	8.68187	12.17322
DIgSILENT	1.94183	1.54792	8.68973	12.17948

The numerical results in Table 9 show that, with respect to the benchmark case, the optimal placement of fixed-step capacitor banks allowed a power losses reduction of 13%, i.e., 1.8193 kW, which is lower in comparison with the phase-swapping solution reported in Table 8. It also has a positive impact on the final grid power losses, and the combination of both approaches for the CSM and the SSM will perhaps yield better results in terms of power loss minimization since both approaches independently allow for reducing this indicator with respect to the benchmark case.

Table 10 presents the numerical comparison between the proposed CSM and SSM presented in Figures 1 and 2.

Table 10. Comparison of solution methodologies for the IEEE 8-bus grid.

	CSM		SSM	
	MATLAB	**DIgSILENT**	**MATLAB**	**DIgSILENT**
Load connections	3, 5, 1, 3, 2, 2, 5	3, 5, 1, 3, 2, 2, 5	3, 5, 1, 3, 4, 2, 5	3, 5, 1, 3, 4, 2, 5
Capacitor banks location	2, 3	2, 3	2, 3	2, 3
Capacitor banks type	3, 1	3, 1	3, 1	3, 1
Phase a (kW)	2.26340	3.22020	3.21842	3.22020
Phase b (kW)	3.21842	3.29553	3.29621	3.29553
Phase c (kW)	3.29621	2.26271	2.26340	2.26271
Total (kW)	8.77804	8.77843	8.77804	8.77843

The numerical results presented in Table 10 allow for noting that:

i. Both solution methodologies found the same objective function value regarding the final grid power losses, i.e., 8.7780 kW. This implies a reduction of about 37.27% with respect to the benchmark case;
ii. For the IEEE 8-bus grid, the CSM and the SSM are equivalent in terms of the final objective function value. However, due to the nonlinearities and non-convexities of the solution space for the studied problems, the final load connections in both solution methods differ from each other.

It is worth mentioning that the SSM and CSM found the same objective function values due to the small size of the solution space for the studied problem in the IEEE 8-bus grid. As demonstrated by the authors of [5] for the optimal phase balancing problem, the solution of the IEEE 8-bus grid is the global optimum, and, given the results obtained by this system, perhaps the size and location of the fixed-step capacitor banks presented in this paper is also optimal.

To demonstrate that the solutions reached with both methodologies in the MATLAB programming environment are equivalent to those of the three-phase power flow approach in the DIgSILENT software, Table 11 lists the voltage magnitudes per phase.

Table 11. Voltage magnitude per phase in the IEEE 8-bus grid after implementing the CSM and/or the SSM.

	MATLAB			**DIgSILENT**		
Node	V_a	V_b	V_c	V_a	V_b	V_c
1	1.00000	1.00000	1.00000	0.99999	0.99999	1.00002
2	0.99801	0.99812	0.99853	0.99800	0.99812	0.99855
3	0.99658	0.99645	0.99796	0.99656	0.99644	0.99798
4	0.99662	0.99650	0.99766	0.99661	0.99649	0.99768
5	0.99773	0.99797	0.99862	0.99772	0.99796	0.99863
6	0.99788	0.99763	0.99874	0.99778	0.99762	0.99869
7	0.99812	0.99825	0.99785	0.99810	0.99824	0.99786
8	0.99667	0.99594	0.99804	0.99665	0.99594	0.99806

In addition, to verify the effect of optimal phase-balancing while considering capacitor banks in three-phase asymmetric networks, the behavior of the voltage profiles per phase is presented in Figure 3. This figure shows the voltage profile for the benchmark case, as well as for the CSM and the SSM.

The behavior of the voltage profile for the IEEE 8-bus grid (Figure 3) allows for making the following remarks. (i) The voltage profile in phase c for the benchmark case (Figure 3a) is the worst profile when compared to phases a and b. However, this is an expected behavior, as c is the most charged phase in the IEEE-8 bus grid. (ii) The plots in Figure 3b,c are identical because the CSM and the SSM found the same objective function value (see Table 10). However, the main result is the fact the all voltages are uniform, i.e., the load redistribution in all the nodes and the reactive power compensation allowed for reaching a more balanced operation at bus 8 for phase b with a minimum voltage of 0.9560 pu.

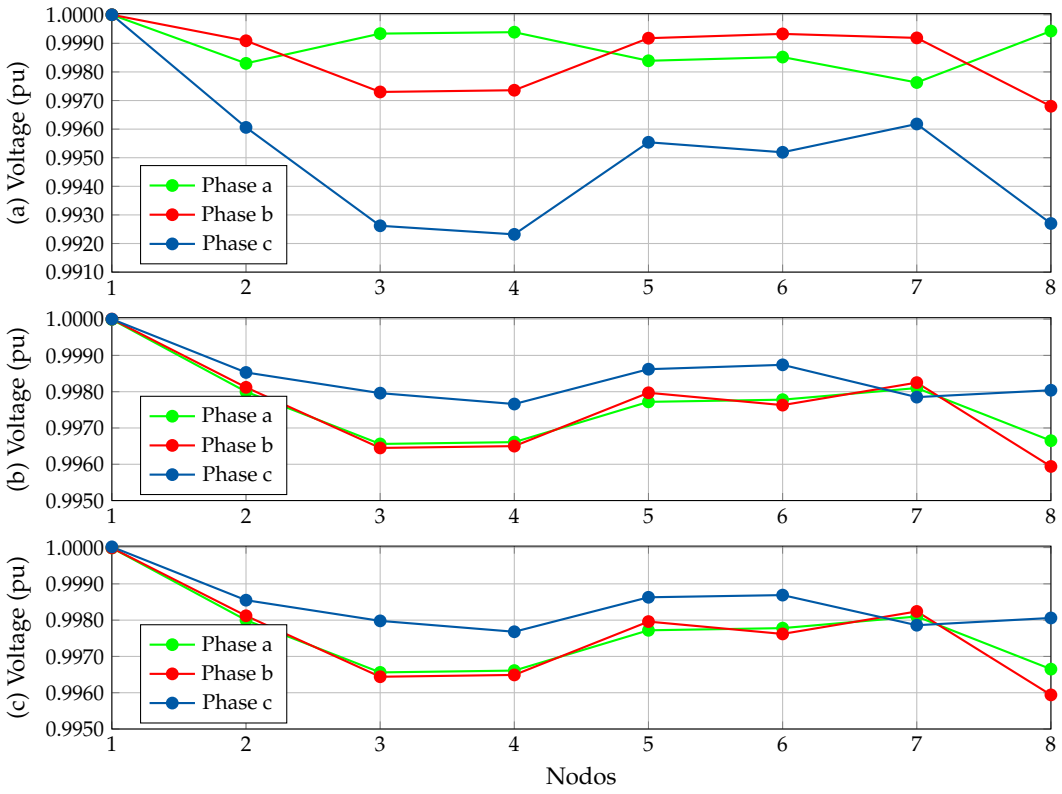

Figure 3. Behavior of the voltage profile in the IEEE 8-bus grid: (**a**) benchmark case; (**b**) CSM; and (**c**) SSM.

6.3. Results for the IEEE 25-Bus Grid

As previously shown with the IEEE 8-bus grid, the first stage of the CSM reorganizes the system loads in order to reduce losses. Table 12 presents the solution to the phase balance problem using the BHO method and its verification in DIgSILENT.

Table 12. Power losses after solving the optimal phase-balancing problem in the IEEE 25-bus grid.

Software	Phase a (kW)	Phase b (kW)	Phase c (kW)	Total (kW)
MATLAB	25.22327	26.40856	20.710.19	72.34203
DIgSILENT	26.73607	25.68264	19.95817	72.37688

The results in Table 12 allow for stating that the evaluation of the optimal solution provided by the BHO algorithm in the IEEE 25-bus grid shows similarities between the MATLAB and the DIgSILENT software, where the minimum value was reached when the three-phase power flow approach was implemented in MATLAB, i.e., in comparison with the Newton–Raphson technique available in the DIgSILENT software. This difference is explained by the convergence errors used in each algorithm, given that the successive approximations method uses the difference between two consecutive voltages, with a maximum error of 1×10^{-10}, whereas the Newton–Raphson approach uses the mismatch between calculated and specified powers, with a precision of 1×10^{-06}.

On the other hand, in order to observe the effect of using fixed-step capacitor banks for shunt reactive power compensation in the IEEE 25-bus grid, Table 13 presents a comparative analysis between MATLAB and DIgSILENT once the BHO was implemented.

Table 13. Power losses after solving the problem regarding optimal reactive power compensation in the IEEE 25-bus grid.

Software	Phase a (kW)	Phase b (kW)	Phase c (kW)	Total (kW)
MATLAB	27.92326	9.48933	16.67151	54.08410
DIgSILENT	27.82905	9.41350	16.78699	54.02954

The results in Table 13 show that the expected power losses in the IEEE 25-bus grid after installing capacitor banks constitute a reduction of about 28.29% with respect to the benchmark case (i.e., 75.4207 kW), which implies that, in this test feeder, shunt reactive power compensation allowed for higher power loss reductions when compared to the phase-balancing case, unlike those reported by the IEEE 8-bus grid. These differences between both test feeders are explained by the nonlinearities and non-convexities of the optimization models that represent both studied problems.

To show the effect of using the CSM in the IEEE 25-bus grid, Table 14 presents the solutions obtained by this approach, which is based on the algorithm depicted in Figure 1, as well as a comparison with the SSM presented in Figure 2.

Table 14. Comparison of solution methodologies for the IEEE 25-bus grid.

	CSM		SSM	
	MATLAB	**DIgSILENT**	**MATLAB**	**DIgSILENT**
Load connections	3, 2, 4, 5, 5, 3, 3, 3, 1, 5, 5, 3, 4, 6, 5, 5, 2, 6, 5, 4, 5, 2, 4, 4		3, 3, 2, 4, 3, 3, 4, 4, 2, 2, 3, 3, 4, 1, 1, 3, 2, 1, 2, 4, 3, 4, 4, 2	
Capacitor banks location	7, 3, 4	7, 3, 4	3, 10, 7	3, 10, 7
Capacitor banks type	2, 1, 1	2, 1, 1	2, 1, 1	2, 1, 1
Phase a (kW)	17.49183	17.47536	18.62210	18.62736
Phase b (kW)	18.40307	18.37194	19.33878	19.25855
Phase c (kW)	15.35355	15.30337	12.17873	12.11915
Total (kW)	51.24846	51.15067	50.13961	50.00506

The results in Table 14 allow for making the following remarks. (i) The CSM allows for finding a final objective function value of about 51.2485 kW, i.e., a reduction of about 32.05% with respect to the benchmark case, while the SSM has a final objective function value of about 50.1396 kW, i.e., a 33.52% reduction in the total grid power losses. (ii) The CSM and the SSM differ in the final set of nodal connections for loads and in the size and location of the fixed-step capacitor banks. However, this is an expected behavior, as the CSM approach focuses on minimizing each problem separately, i.e., the first stage solves the phase-swapping problem, and the second stage solves the optimal reactive power compensation problem. Nevertheless, the solution to the second problem is completely conditioned by that obtained in the first stage. In contrast, the SSM method addresses both problems simultaneously, which implies no conditioning by the solution of an initial stage, thus allowing for a better exploration and exploitation of the solution space.

To confirm that the solutions reached with both methodologies in the MATLAB programming environment are equivalent to the solution of the three-phase power flow approach obtained via the DIgSILENT software, Table 15 lists voltage magnitudes per phase.

Furthermore, in order to verify the effect of optimal phase-balancing while considering capacitor banks in three-phase asymmetric networks, the per-phase behavior of the voltage profiles is presented in Figure 4. This figure shows the voltage profile of the benchmark case, as well as that of the SSM, since, as observed in Table 15, it yields better objective function values in comparison with the CSM.

Table 15. Voltage magnitude per phase in the IEEE 25-bus grid after implementing the CSM and/or the SSM.

	CSM						SSM					
	MATLAB			DIgSILENT			MATLAB			DIgSILENT		
Node	V_a	V_b	V_c	V_a	V_b	V_c	V_a	V_b	V_c	V_a	V_b	V_c
1	1.00000	1.00000	1.00000	1.00000	1.00000	0.99999	1.00000	1.00000	1.00000	0.99999	1.00000	1.00001
2	0.99113	0.99041	0.99332	0.99077	0.99088	0.99306	0.99011	0.99010	0.99480	0.98968	0.98970	0.99456
3	0.98923	0.98867	0.99184	0.98881	0.98827	0.99153	0.98819	0.98782	0.99383	0.98769	0.98738	0.99356
4	0.98847	0.98831	0.99153	0.98801	0.98788	0.99120	0.98610	0.98589	0.99242	0.98560	0.98545	0.99214
5	0.98761	0.98761	0.99052	0.98715	0.98718	0.99019	0.98501	0.98505	0.99180	0.98451	0.98461	0.99153
6	0.98457	0.98310	0.98709	0.98404	0.98261	0.98670	0.98246	0.98329	0.98928	0.98183	0.98274	0.98892
7	0.97896	0.97784	0.98241	0.97827	0.97720	0.98191	0.97680	0.97757	0.98526	0.97597	0.97684	0.98478
8	0.98442	0.98077	0.98598	0.98389	0.98028	0.98560	0.98034	0.98330	0.98775	0.97971	0.98275	0.98739
9	0.97379	0.97217	0.97769	0.97310	0.97153	0.97718	0.97324	0.97362	0.98250	0.97230	0.97279	0.98194
10	0.96985	0.96834	0.97372	0.96915	0.96769	0.97321	0.97157	0.97072	0.98062	0.97052	0.96979	0.98000
11	0.96800	0.96645	0.97183	0.96730	0.96580	0.97132	0.96990	0.96850	0.97893	0.96885	0.96757	0.97830
12	0.96707	0.96552	0.97077	0.96636	0.96487	0.97026	0.96895	0.96743	0.97803	0.96790	0.96650	0.97740
13	0.96730	0.96541	0.97124	0.96660	0.96476	0.97072	0.96920	0.96746	0.97834	0.96815	0.96653	0.97771
14	0.97606	0.97539	0.98001	0.97536	0.97474	0.97950	0.97374	0.97453	0.98364	0.97281	0.97374	0.98307
15	0.97599	0.97528	0.97993	0.97529	0.97464	0.97942	0.97364	0.97447	0.98356	0.97281	0.97374	0.98307
16	0.97780	0.97736	0.98143	0.97711	0.97671	0.98092	0.97595	0.97717	0.98393	0.97512	0.97644	0.98344
17	0.97453	0.97444	0.97829	0.97383	0.97380	0.97778	0.97216	0.97285	0.98271	0.97133	0.97212	0.98222
18	0.98510	0.98463	0.98739	0.98467	0.98423	0.98708	0.98426	0.98314	0.98986	0.98376	0.98269	0.98959
19	0.98344	0.98312	0.98583	0.98301	0.98272	0.98551	0.98272	0.98146	0.98835	0.98222	0.98102	0.98808
20	0.98362	0.98346	0.98606	0.98319	0.98306	0.98575	0.98306	0.98164	0.98859	0.98255	0.98119	0.98832
21	0.98251	0.98219	0.98453	0.98208	0.98179	0.98410	0.98164	0.98019	0.98754	0.98113	0.97974	0.98726
22	0.98015	0.97995	0.98179	0.97972	0.97955	0.98147	0.97924	0.97745	0.98534	0.98874	0.97700	0.98507
23	0.98719	0.98701	0.98989	0.98673	0.98658	0.98955	0.98411	0.98455	0.99149	0.98361	0.98410	0.99122
24	0.98602	0.98688	0.98888	0.98555	0.98645	0.98855	0.98303	0.98440	0.99039	0.98253	0.98396	0.99012
25	0.98568	0.98666	0.98871	0.98521	0.98623	0.98837	0.98287	0.98417	0.99006	0.98237	0.98373	0.98978

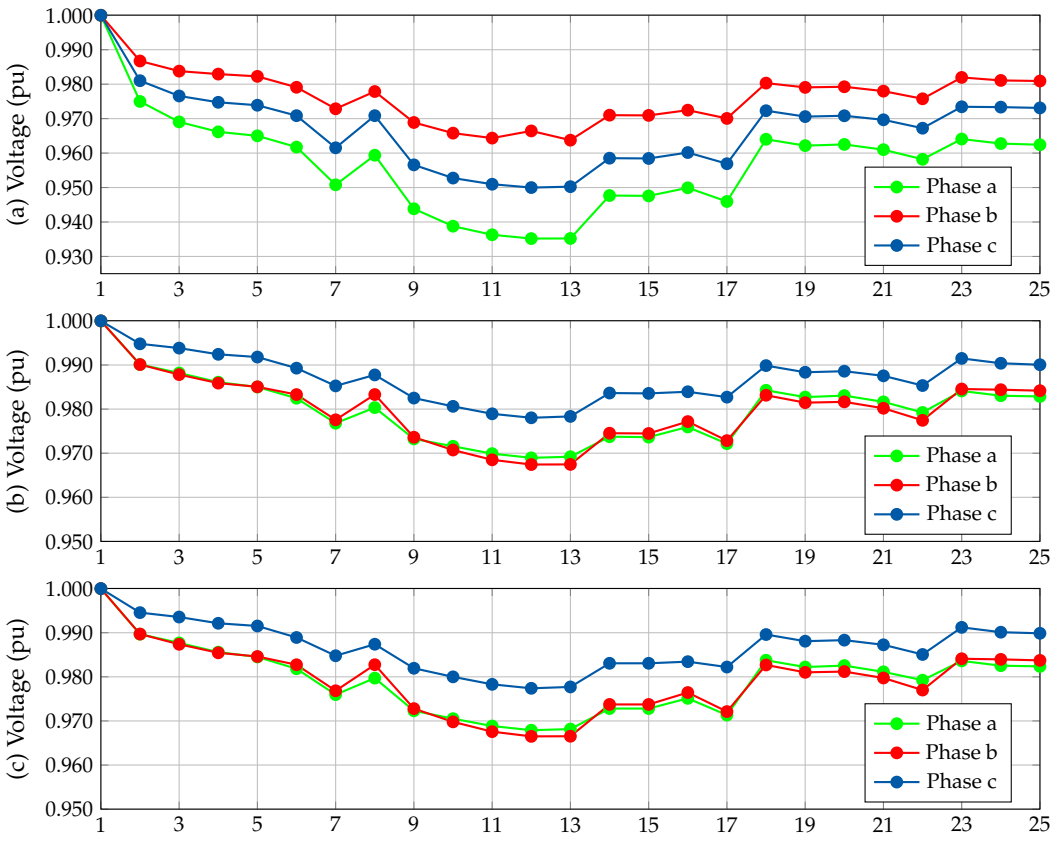

Figure 4. Behavior of the voltage profile in the IEEE 25-bus grid: (**a**) benchmark case; (**b**) MATLAB; and (**c**) DIgSILENT.

The behavior of the voltage profile for the IEEE 25-bus grid in Figure 4 allows for observing that: (i) the minimum voltage of the benchmark case is defined by phase at node 13, with a magnitude of 0.9584 pu, i.e., a voltage regulation of about 4.16% (see Figure 4a); and (ii) after implementing the solution provided by the SSM, all the voltage profiles in phases b and c become similar, which is caused by the simultaneous effect of phase-swapping and shunt reactive power compensation (see Figure 4b,c). However, the worst voltage profile now corresponds to phase b at node 13, with a magnitude of about 0.9675 pu, which means a regulation of about 3.25%.

6.4. Complementary Analysis

To summarize, the main results regarding the reductions in the total grid power losses are presented in Table 16 for the cases in which the phase-balancing problem and the optimal location of capacitor banks are implemented separately, as well as when the cascade and solution methodologies are employed.

The results in Table 16 reveal the following: (i) When the phase-balancing problem and the optimal selection and location of capacitor banks are solved independently, important variations occur in the expected energy loss reductions, and it is not possible to generalize a tendency. As explained in previous sections, this can be attributed to the nonlinearities and non-convexities of both problems, in addition to the particularities of each test feeder, i.e., the number of nodes, branch impedances, and longitudes, the total power load, and the per-phase unbalanced load. (ii) It is evident that the combination of the phase-balancing problem with the selection and location of shunt capacitors in both methodologies (i.e., CSM and SSM) allows for better improvements in the final objective function when compared to the separate use of each approach. (iii) There is a need to explore alternative solution methods with convex approximations or new combinatorial optimizers in order to validate the effectiveness of the BHO, which constitutes a research opportunity that remains open for future studies.

Table 16. Percentage analysis of the effect of using capacitors and phase-balancing in three-phase asymmetric networks.

IEEE 8-Bus Grid		
Approach	**Losses (kW)**	**Reduction (%)**
Benchmark case	13.99252	0.00
Phase-balancing only	10.58686	24.34
Capacitors only	12.17322	13.00
CSM	8.77804	37.27
SSM	8.77804	37.27
IEEE 25-bus grid		
Approach	**Losses (kW)**	**Reduction (%)**
Benchmark case	75.42059	0.00
Phase-balancing only	72.34203	4.08
Capacitors only	54.08410	28.29
CSM	51.24846	32.05
SSM	50.13961	33.52

7. Conclusions

This paper addressed two classical engineering problems concerning distribution networks. The first problem involved optimal phase-swapping in three-phase asymmetric distribution networks, and the second was optimal shunt reactive power compensation using fixed-step capacitor banks. A master–slave solution methodology was implemented to solve both problems, based on applying the BHO approach combined with the successive approximations power flow method. The main contribution of this research is its proposal and application of two solution methodologies to solve both optimization problems. The

first approach was the CSM, where the first stage solves the phase-balancing problem, and the second one solves the shunt reactive power compensation problem by fixing the set of load configurations provided by the solution of the first stage. The second approach was the SSM, which solves both studied problems simultaneously.

Numerical results in the IEEE 8- and 25-bus grids demonstrated the following:

i. For the IEEE 8-bus grid, both solution methodologies found the same value regarding the total grid power losses, with a reduction of about 32.27% concerning the benchmark case. The size of the solution space explains the coincidence in both solutions in this test feeder, which can be regarded as undersized for real distribution grids. This implies that an efficient optimization method can find the optimal global solution.
ii. In the IEEE 25-bus grid, the solution of the SSM was better than that of the CSM by about 1.1089 kW. This result is expected since the solution space increased in size. The SSM is more capable of exploring and exploiting the solution space, as the solution of the phase-balancing problem does not condition it.
iii. More research is required to include, within the proposed optimization model, the possibility of having shunt reactive power compensation per phase (unbalanced reactive power compensation) combined with the phase-balancing solution employing CSM and SSM. In addition, a complete comparative analysis with different combinatorial optimizers is needed in order to verify the effectiveness of the proposed solution methodology addressed in this research.

In future works, it will be possible to conduct the following studies: (i) applying new combinatorial optimization methods to deal with the studied problems while using the SSM; (ii) considering daily load profiles and different end-users (residential, industrial, and commercial) in the optimization model; (iii) allocating static distribution compensators in three-phase grids for hourly reactive power control according to the grid requirements; and (iv) evaluating additional objective functions while considering daily demand curves, as is the case of the total required investments in compensation devices and grid interventions and the expected yearly reduction costs regarding energy losses.

Author Contributions: Conceptualization, O.D.M.; Methodology, D.F.A.M.-G., I.D.R.-R. and O.D.M.; Software, D.F.A.M.-G. and I.D.R.-R.; Validation, D.F.A.M.-G. and I.D.R.-R.; Formal analysis, O.D.M.; Investigation, I.D.R.-R.; Resources, O.D.M.; Writing—original draft, D.F.A.M.-G., I.D.R.-R. and O.D.M.; Writing—review & editing, O.D.M.; Visualization, O.D.M.; Supervision, O.D.M.; Project administration, O.D.M.; Funding acquisition, O.D.M. All authors have read and agreed to the published version of the manuscript.

Funding: This research received no external funding.

Institutional Review Board Statement: Not applicable.

Informed Consent Statement: Not applicable.

Conflicts of Interest: The authors declare no conflict of interest.

References

1. Chowdhury, P.K.R.; Weaver, J.E.; Weber, E.M.; Lunga, D.; LeDoux, S.T.M.; Rose, A.N.; Bhaduri, B.L. Electricity consumption patterns within cities: Application of a data-driven settlement characterization method. *Int. J. Digit. Earth* **2019**, *13*, 119–135. [CrossRef]
2. Mutumba, G.S.; Odongo, T.; Okurut, N.F.; Bagire, V. A survey of literature on energy consumption and economic growth. *Energy Rep.* **2021**, *7*, 9150–9239. [CrossRef]
3. Nogueira, T.; Sousa, E.; Alves, G.R. Electric vehicles growth until 2030: Impact on the distribution network power. *Energy Rep.* **2022**, *8*, 145–152. [CrossRef]
4. Arefi, A.; Shahnia, F.; Ledwich, G. (Eds.) *Electric Distribution Network Management and Control*; Springer: Singapore, 2018. [CrossRef]
5. Cortés-Caicedo, B.; Avellaneda-Gómez, L.S.; Montoya, O.D.; Alvarado-Barrios, L.; Chamorro, H.R. Application of the Vortex Search Algorithm to the Phase-Balancing Problem in Distribution Systems. *Energies* **2021**, *14*, 1282. . [CrossRef]
6. Arefi, A.; Olamaei, J.; Yavartalab, A.; Keshtkar, H. Loss reduction experiences in electric power distribution companies of Iran. *Energy Procedia* **2012**, *14*, 1392–1397. [CrossRef]

7. Abagiu, S.; Lepadat, I.; Helerea, E. Solutions for energy losses reduction in power networks with renewable energy sources. In Proceedings of the 2016 International Conference on Applied and Theoretical Electricity (ICATE), Craiova, Romania, 6–8 October 2016. [CrossRef]
8. Hesaroor, K.; Das, D. Annual energy loss reduction of distribution network through reconfiguration and renewable energy sources. *Int. Trans. Electr. Energy Syst.* **2019**, *29*, e12099. [CrossRef]
9. Chernykh, A.G.; Barykina, Y.N.; Morozevich, O.A. Development of methods for minimizing energy losses in electrical networks. *IOP Conf. Ser. Earth Environ. Sci.* **2022**, *1070*, 012006. [CrossRef]
10. Prakash, D.; Lakshminarayana, C. Optimal siting of capacitors in radial distribution network using Whale Optimization Algorithm. *Alex. Eng. J.* **2017**, *56*, 499–509. [CrossRef]
11. Sulaiman, M.H.; Mustaffa, Z. Optimal placement and sizing of FACTS devices for optimal power flow using metaheuristic optimizers. *Results Control Optim.* **2022**, *8*, 100145. [CrossRef]
12. Valencia, A.; Hincapie, R.A.; Gallego, R.A. Optimal location, selection, and operation of battery energy storage systems and renewable distributed generation in medium–low voltage distribution networks. *J. Energy Storage* **2021**, *34*, 102158. [CrossRef]
13. Ghiasi, M. Detailed study, multi-objective optimization, and design of an AC-DC smart microgrid with hybrid renewable energy resources. *Energy* **2019**, *169*, 496–507. [CrossRef]
14. Salau, A.O.; Gebru, Y.W.; Bitew, D. Optimal network reconfiguration for power loss minimization and voltage profile enhancement in distribution systems. *Heliyon* **2020**, *6*, e04233. [CrossRef]
15. Askarzadeh, A. Capacitor placement in distribution systems for power loss reduction and voltage improvement: A new methodology. *IET Gener. Transm. Distrib.* **2016**, *10*, 3631–3638. [CrossRef]
16. Ghiasi, M.; Olamaei, J. Optimal capacitor placement to minimizing cost and power loss in Tehran metro power distribution system using ETAP (A case study). *Complexity* **2016**, *21*, 483–493. [CrossRef]
17. Tamilselvan, V.; Jayabarathi, T.; Raghunathan, T.; Yang, X.S. Optimal capacitor placement in radial distribution systems using flower pollination algorithm. *Alex. Eng. J.* **2018**, *57*, 2775–2786. [CrossRef]
18. Devabalaji, K.; Yuvaraj, T.; Ravi, K. An efficient method for solving the optimal sitting and sizing problem of capacitor banks based on cuckoo search algorithm. *Ain Shams Eng. J.* **2018**, *9*, 589–597. [CrossRef]
19. Taher, S.A.; Bagherpour, R. A new approach for optimal capacitor placement and sizing in unbalanced distorted distribution systems using hybrid honey bee colony algorithm. *Int. J. Electr. Power Energy Syst.* **2013**, *49*, 430–448. [CrossRef]
20. Ogita, Y.; Mori, H. Parallel Dual Tabu Search for Capacitor Placement in Smart Grids. *Procedia Comput. Sci.* **2012**, *12*, 307–313. [CrossRef]
21. Faiz, M.; Chang, A.Q.; Memon, N.; Pathan, A.Z.U. Optimal Capacitor Placement Using Tabu Search Algorithm to Improve the Operational Efficiency in GEPCO Network. *Int. J. Electr. Electron. Eng.* **2021**, *8*, 1–5. [CrossRef]
22. Gil-González, W.; Montoya, O.D.; Rajagopalan, A.; Grisales-Noreña, L.F.; Hernández, J.C. Optimal Selection and Location of Fixed-Step Capacitor Banks in Distribution Networks Using a Discrete Version of the Vortex Search Algorithm. *Energies* **2020**, *13*, 4914. [CrossRef]
23. Khan, N.A.; Ghosh, S.; Ghoshal, S.P. Binary Gravitational Search based Algorithm for Optimum Siting and Sizing of DG and Shunt Capacitors in Radial Distribution Systems. *Energy Power Eng.* **2013**, *05*, 1005–1010. [CrossRef]
24. Zadeh, A.Z.; Andami, H.; Talavat, V.; Ebrahimi, J. Optimal Capacitor Placement in the Unbalanced Distribution Networks Contaminated by Harmonic through Imperialist Competitive Algorithm. *Res. J. Appl. Sci. Eng. Technol.* **2014**, *7*, 1230–1235. [CrossRef]
25. Murty, V.; Kumar, A. Capacitor Allocation in Unbalanced Distribution System under Unbalances and Loading Conditions. *Energy Procedia* **2014**, *54*, 47–74. [CrossRef]
26. Echeverri, M.G.; Rendón, R.A.G.; Lezama, J.M.L. Optimal Phase Balancing Planning for Loss Reduction in Distribution Systems using a Specialized Genetic Algorithm. *Ing. Cienc.* **2012**, *8*, 121–140. [CrossRef]
27. Khodr, H.; Zerpa, I.; de Jesu's, P.D.O.; Matos, M. Optimal Phase Balancing in Distribution System Using Mixed-Integer Linear Programming. In Proceedings of the 2006 IEEE/PES Transmission & Distribution Conference and Exposition: Latin America, Caracas, Venezuela, 15–18 August 2006. [CrossRef]
28. El Hassan, M.; Najjar, M.; Tohme, R. A Practical Way to Balance Single Phase Loads in a Three Phase System at Distribution and Unit Level. *Renew. Energy Power Qual. J.* **2022**, *20*, 173–177. [CrossRef]
29. Mansani, S.; Udaykumay, R.Y. An optimal phase balancing technique for unbalanced three-phase secondary distribution systems. In Proceedings of the 2016 IEEE 7th Power India International Conference (PIICON), Bikaner, India, 25–27 November 2016. [CrossRef]
30. Alhmoud, L.; Nawafleh, Q.; Merrji, W. Three-Phase Feeder Load Balancing Based Optimized Neural Network Using Smart Meters. *Symmetry* **2021**, *13*, 2195. [CrossRef]
31. Cruz-Reyes, J.L.; Salcedo-Marcelo, S.S.; Montoya, O.D. Application of the Hurricane-Based Optimization Algorithm to the Phase-Balancing Problem in Three-Phase Asymmetric Networks. *Computers* **2022**, *11*, 43. [CrossRef]
32. Pandey, A.; Jereminov, M.; Wagner, M.R.; Bromberg, D.M.; Hug, G.; Pileggi, L. Robust Power Flow and Three-Phase Power Flow Analyses. *IEEE Trans. Power Syst.* **2019**, *34*, 616–626. [CrossRef]
33. Garces, A. A Linear Three-Phase Load Flow for Power Distribution Systems. *IEEE Trans. Power Syst.* **2016**, *31*, 827–828. [CrossRef]

34. Marini, A.; Mortazavi, S.; Piegari, L.; Ghazizadeh, M.S. An efficient graph-based power flow algorithm for electrical distribution systems with a comprehensive modeling of distributed generations. *Electr. Power Syst. Res.* **2019**, *170*, 229–243. [CrossRef]
35. Shen, T.; Li, Y.; Xiang, J. A Graph-Based Power Flow Method for Balanced Distribution Systems. *Energies* **2018**, *11*, 511. [CrossRef]
36. Gnanambal, K.; Marimuthu, N.; Babulal, C. Three-phase power flow analysis in sequence component frame using Hybrid Particle Swarm Optimization. *Appl. Soft Comput.* **2011**, *11*, 1727–1734. [CrossRef]
37. Singh, M.K.; Gupta, A.R.; Kumar, A. Analysis of Unbalanced Radial Distribution System with SVR and Impact of Phase Shifter Angle considering Time Varying Loads. *Smart Sci.* **2021**, 1–16. [CrossRef]
38. Swapna, M.; Udaykumar, R.Y. An algorithm for optimal phase balancing of secondary distribution systems at each node. In Proceedings of the 2016 IEEE PES 13th International Conference on Transmission & Distribution Construction, Operation & Live-Line Maintenance (ESMO), Columbus, OH, USA, 12–15 September 2016. [CrossRef]
39. Kumar, S.; Datta, D.; Singh, S.K. Black Hole Algorithm and Its Applications. In *Studies in Computational Intelligence*; Springer International Publishing: Cham, Switzerland, 2014; pp. 147–170. [CrossRef]
40. Abualigah, L.; Elaziz, M.A.; Sumari, P.; Khasawneh, A.M.; Alshinwan, M.; Mirjalili, S.; Shehab, M.; Abuaddous, H.Y.; Gandomi, A.H. Black hole algorithm: A comprehensive survey. *Appl. Intell.* **2022**, *52*, 11892–11915. [CrossRef]
41. Velasquez, O.S.; Montoya, O.D.; Garrido, V.M.; Grisales, L.F. Optimal Power Flow in Direct-Current Power Grids via Black Hole Optimization. *Adv. Electr. Electron. Eng.* **2019**, *17, 24–32* . [CrossRef]
42. Arenas-Acuña, C.A.; Rodriguez-Contreras, J.A.; Montoya, O.D.; Rivas-Trujillo, E. Black-Hole Optimization Applied to the Parametric Estimation in Distribution Transformers Considering Voltage and Current Measures. *Computers* **2021**, *10*, 124. [CrossRef]
43. Hatamlou, A. Black hole: A new heuristic optimization approach for data clustering. *Inf. Sci.* **2013**, *222*, 175–184. [CrossRef]
44. Ramana, T.; Ganesh, V.; Sivanagaraju, S. Distributed Generator Placement In addition, Sizing in Unbalanced Radial Distribution System. *Cogener. Distrib. Gener. J.* **2010**, *25*, 52–71. [CrossRef]
45. Ganesh, S.; Perilla, A.; Torres, J.R.; Palensky, P.; van der Meijden, M. Validation of EMT Digital Twin Models for Dynamic Voltage Performance Assessment of 66 kV Offshore Transmission Network. *Appl. Sci.* **2020**, *11*, 244. [CrossRef]
46. Bifaretti, S.; Bonaiuto, V.; Pipolo, S.; Terlizzi, C.; Zanchetta, P.; Gallinelli, F.; Alessandroni, S. Power Flow Management by Active Nodes: A Case Study in Real Operating Conditions. *Energies* **2021**, *14*, 4519. [CrossRef]